



PRESSURE AND PRESSURE ANALYSIS FOR DOUBLE-PERMEABILITY SYSTEMS WITHOUT TYPE-CURVE MATCHING

Freddy Humberto Escobar, James Vega and Maiver Ramiro Diaz
 Universidad Surcolombiana, Avenida Pastrana, Cra 1, Neiva, Huila, Colombia
 E-Mail: fescobar@usco.edu.co

ABSTRACT

Often, double-porosity models have been widely used for characterization of naturally fractured reservoirs. However, there is a need of using more complex mathematical models such as double-permeability to better describe fractured reservoirs. It has been noticed that the behavior of such reservoirs do not have the classical unit-slope during the transition period in double-porosity systems and the homogeneous behavior is also different since the second radial flow regime has a lower value as the matrix permeability contributes to the flow capacity. In this work, a model previously presented in the literature is used to understand the pressure and pressure derivative behavior of double-permeability systems with the purpose of developing a practical and easy methodology for their characterization which was successfully tested and verified with synthetic cases.

Keywords: double permeability, interporosity flow parameter, dimensionless storage coefficient, flo capacity ratio, TDS technique.

1. INTRODUCTION

Modeling and characterizing naturally occurring formations is a challenging milestone for engineers in the oil industry due to geology aspects and complex flow nature. However, such reservoirs contain a significant amount of oil and gas reserves around the globe.

The pioneer research on simulation of naturally fractured reservoirs was presented by Barenblatt, Zheltov and Kochina (1960) which used the concept of double-porosity systems. Three years later, Warren and Root (1963) extended their model to well test analysis. Their system consisted of two media: blocks of matrix and a network of fractures. On one side, the matrix blocks contain most of the fluid volume and constitute a source of fluid for the fracture net. On the other side, fractures possess a relative small volume but a high permeability which enables fluid flow towards the well.

For cases of high matrix permeability, the fluid from the matrix moves perpendicularly towards the fractures and parallel to the stratum in the direction of the well. This is recognized as double permeability model and was introduced by Hill and Thomas (1985). Then, Bremer, Winston and Vela (1985) developed a mathematical model and applied conventional analysis for well test interpretation. Also, Ehlig-Economides and Ayoub (1986) presented a mathematical model considering two formations separated by a thin layer of very low permeability. They also used the pressure derivative function and presented a type-curve matching well test interpretation procedure. A much more complex model was also presented by Lir and Chen (1987) with neither pressure behavior nor interpretation technique.

Besides the λ and ω parameters introduced by Warren and Root (1963), a third one, κ , which represents the matrix-fracture flow capacity ratio, is introduced for the double-permeability model. The main objective of this work is to provide direct expression to estimate such parameters.

2. MATHEMATICAL FORMULATION

The dimensionless quantities introduced by Bremer *et al.* (1985) are:

$$P_{1D,2D} = \frac{(k_1 h_1 + k_2 h_2)}{\alpha_p q \mu} (P_i - P_{1,2}) \quad (1)$$

$$t_{DV} = \frac{\alpha_i (k_1 h_1 + k_2 h_2) t}{[(\phi c_i h)_1 + (\phi c_i h)_2] \mu r_w^2} \quad (2)$$

$$r_D = \frac{r}{r_w} \quad (3)$$

$$\kappa = \frac{k_1 h_1}{k_1 h_1 + k_2 h_2} \quad (4)$$

$$\omega = \frac{(\phi c_i h)_1}{(\phi c_i h)_1 + (\phi c_i h)_2} \quad (5)$$

$$\lambda = \frac{r_w^2}{(k_1 h_1 + k_2 h_2)} \frac{k_v}{\Delta h} \quad (6)$$

and;

$$C_{DV} = \frac{\alpha_c C}{[(\phi c_i h)_1 + (\phi c_i h)_2] r_w^2} \quad (7)$$

Bremer *et al.* (1986) presented pressure solutions in the Laplace space for layers 1 and 2, Equations 8 and 12. These solutions were used in this work.



$$\bar{P}_{1D} = (1/\ell - C_{DV} \sqrt{\bar{P}_{wD}}) \times \left\{ \frac{1}{\kappa(a_2 - a_1)} \left[\frac{a_2 K_0(\sigma_2 r_D)}{\sigma_2 K_1(\sigma_2)} - \frac{a_1 K_0(\sigma_1 r_D)}{\sigma_1 K_1(\sigma_1)} \right] \right\} \quad (8)$$

$$\sigma_{1,2}^2 = \frac{1}{2} \left[\frac{(1-\omega)\ell + \lambda}{1-\kappa} + \frac{\omega\ell + \lambda}{\kappa} \right] \pm \frac{1}{2} \left[\left(\frac{(1-\omega)\ell + \lambda}{1-\kappa} - \frac{\omega\ell + \lambda}{\kappa} \right)^2 + \frac{4\lambda^2}{\kappa(1-\kappa)} \right]^{1/2} \quad (10)$$

Where:

$$K_1^0(z) = K_0(z) / [zK_1(z)] \quad (11)$$

$$a_{1,2} = \frac{(1-\kappa)}{\lambda} \left[\frac{(1-\omega)\ell + \lambda}{1-\kappa} - \sigma_{1,2}^2 \right] \quad (9)$$

$$\bar{P}_{2D} = (1/\ell - C_{DV} \sqrt{\bar{P}_{wD}}) \times \left\{ \frac{1}{\kappa(a_2 - a_1)} \left[\frac{K_0(\sigma_2 r_D)}{\sigma_2 K_1(\sigma_2)} - \frac{K_0(\sigma_1 r_D)}{\sigma_1 K_1(\sigma_1)} \right] \right\} \quad (12)$$

Table-1. Reservoir, fluid and flow properties for simulation and examples.

Parameter	Simulation	Example-1	Example-2
q , STB/D	500	800	500
B_{os} , rb/STB	1.15	1.4	1.5
μ_o , cp	2.5	20	15
c_t , 1/psi	4×10^{-6}	1×10^{-6}	1×10^{-6}
h , ft	115	120	150
ϕ , %	20	22	10
r_w , ft	0.5		
P_b , psi	5000	5000	3000
k , md	50	160	150
s	0		
C , bbl/psi	0	0	0.2
λ	$1 \times 10^{-3} - 1 \times 10^{-7}$	1×10^{-5}	1×10^{-6}
ω	0.005-0.99	0.4	0.06
κ	0.1-0.99	0.7	0.5

3. INTERPRETATION METHODOLOGY

The nature of the interpretation technique follows the philosophy of the *TDS* technique proposed by Tiab (1993). In order to study the pressure and pressure derivative behavior, several pressure tests for different combinations of ω, λ and κ were run with the information presented in the second column of Table-1.

Notice in Figures 1 to 3 that as κ becomes smaller the matrix permeability increases and the homogeneous

radial flow pressure derivative decreases indicating that the total permeability has increased. In Figure-4, a comparison between the double porosity and double permeability model is given. A double-porosity system is a special case of a double-permeability system when $\kappa = 1$. For such case (the highest possible value of κ used for the simulation was 0.99), the transition behavior takes longer in double-permeability case since the mass transfer is delayed due to the complexity of the system.

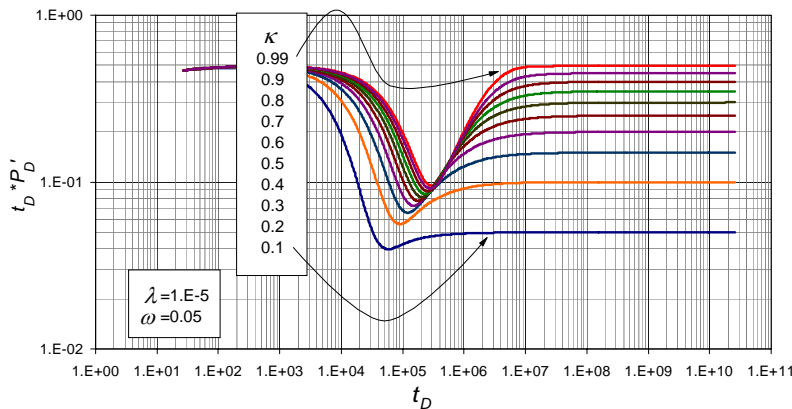


Figure-1. Pressure derivative behavior for $\omega = 0.05$, $\lambda = 1 \times 10^{-5}$ and $0.1 \leq \kappa \leq 0.99$.

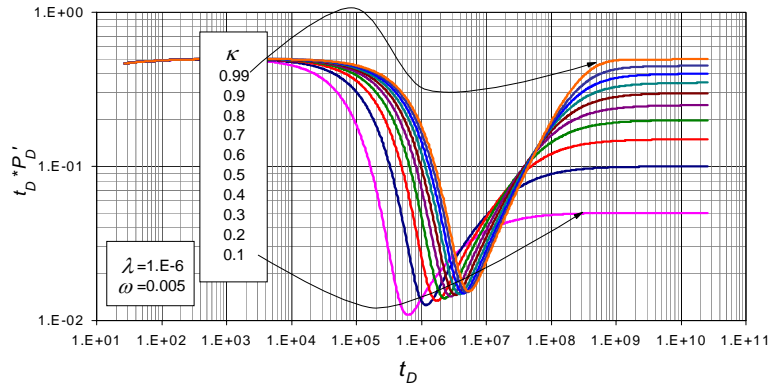


Figure-2. Pressure derivative behavior for $\omega = 0.005$, $\lambda = 1 \times 10^{-6}$ and $0.1 \leq \kappa \leq 0.99$.

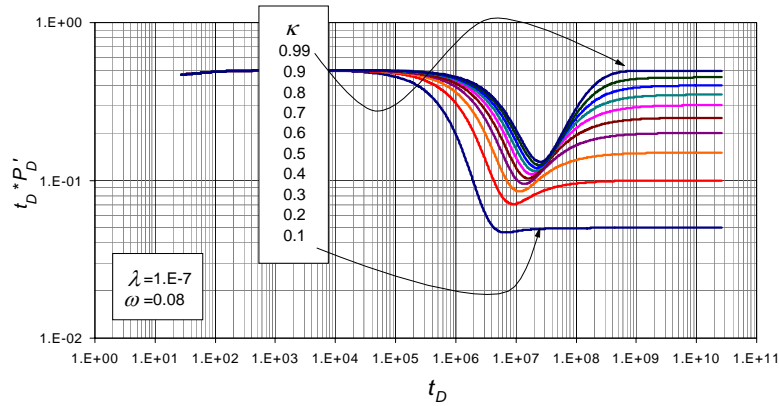


Figure-3. Pressure derivative behavior for $\omega = 0.08$, $\lambda = 1 \times 10^{-7}$ and $0.1 \leq \kappa \leq 0.99$.

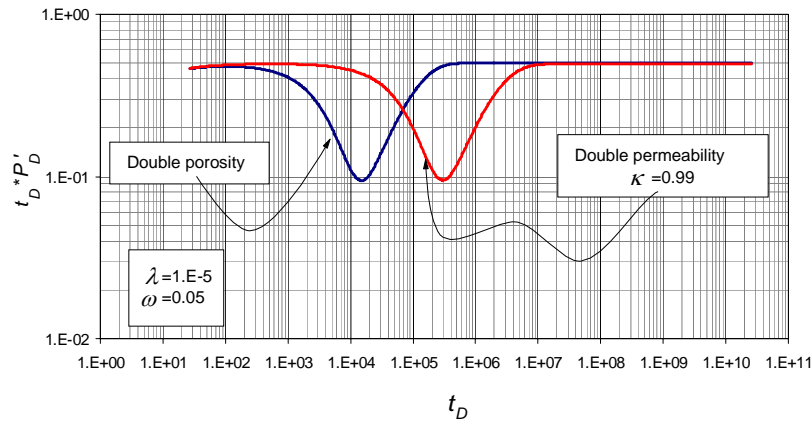


Figure-4. Comparison of double porosity and double permeability models for $\omega = 0.05$, $\lambda = 1 \times 10^{-5}$ and $\kappa = 0.99$.

Using regression analysis was possible to find an expression to estimate κ from the ratio of the two radial pressure derivative values:

$$\ln(\kappa) = 0.00073002267 + 0.999971542 * \ln\left(\frac{(t^* \Delta P')_{r2}}{(t^* \Delta P')_{r1}}\right) - \frac{0.00030874828}{\omega^{0.5}} \quad (13)$$

Another correlation using the ratio between the minimum and second radial derivative was obtained for estimating the dimensionless storage coefficient, ω ,



$$\ln(\omega) = 13.46 - 81.83(\kappa) + 80.26(\kappa)^{0.5} * \ln(\kappa) + 16.78 \ln(\kappa) + 39.06 \exp(-\kappa) + 48.17 \left\{ \frac{(t^* \Delta P')_{\min}}{(t^* \Delta P')_{r_2}} \right\} - 22.88 \left\{ \frac{(t^* \Delta P')_{\min}}{(t^* \Delta P')_{r_2}} \right\}^{1.5} + 11.46 \left\{ \frac{(t^* \Delta P')_{\min}}{(t^* \Delta P')_{r_2}} \right\}^{0.5} + 46.86 \exp\left(-\left\{ \frac{(t^* \Delta P')_{\min}}{(t^* \Delta P')_{r_2}} \right\}\right) \tag{14}$$

Some other expressions for κ as a function of ω are presented in Table-2. These correlations use the ratio of the first radial and second radial (homogeneous-acting behavior) pressure derivatives. Since the influence of ω is very similar in double-porosity and double-permeability, the relationships presented by Engler and Tiab (1996) which use the ratio between the radial flow and minimum pressure derivatives and beginning and ending of the radial flow regimes (Equations 12 to 15) can be used. The following equation was found for the determination of κ ,

$$\lambda = \frac{\kappa + kte}{t_{D\min}} \ln\left(\frac{1}{\omega}\right) \tag{15}$$

Where the constant, kte , is found graphically from Figure-5.

Table-2. Equation of κ as a function of ω and the ratio of the radial pressure derivatives.

ω	Equation
0.005	$\kappa = 0.998739(t^* \Delta P')_{r_2} / (t^* \Delta P')_{r_1} - 0.0002501$
0.05	$\kappa = 0.999891(t^* \Delta P')_{r_2} / (t^* \Delta P')_{r_1} - 0.0000115$
0.08	$\kappa = 1.000066(t^* \Delta P')_{r_2} / (t^* \Delta P')_{r_1} + 0.0000056$
0.2	$\kappa = 1.000024(t^* \Delta P')_{r_2} / (t^* \Delta P')_{r_1} - 0.00000001$
0.4	$\kappa = 1.0000078(t^* \Delta P')_{r_2} / (t^* \Delta P')_{r_1} - 0.0000015$
0.8	$\kappa = 1.0000306(t^* \Delta P')_{r_2} / (t^* \Delta P')_{r_1} - 0.0000332$
0.99	$\kappa = 1.0000235(t^* \Delta P')_{r_2} / (t^* \Delta P')_{r_1} - 0.0000355$

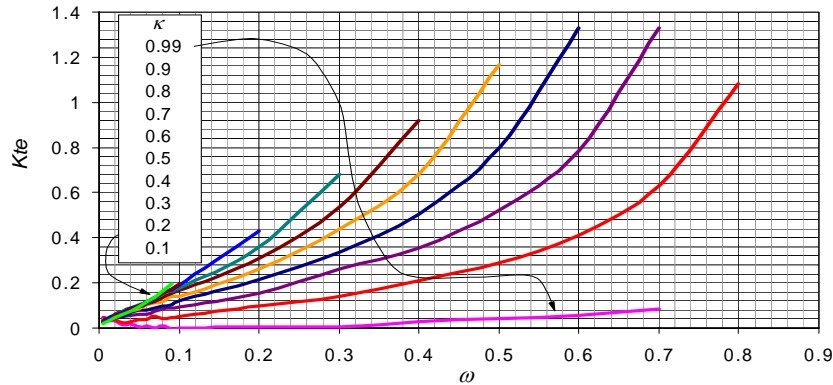


Figure-5. Graphical correlation for estimating the value of λ . $0.1 \leq \kappa \leq 0.99$.

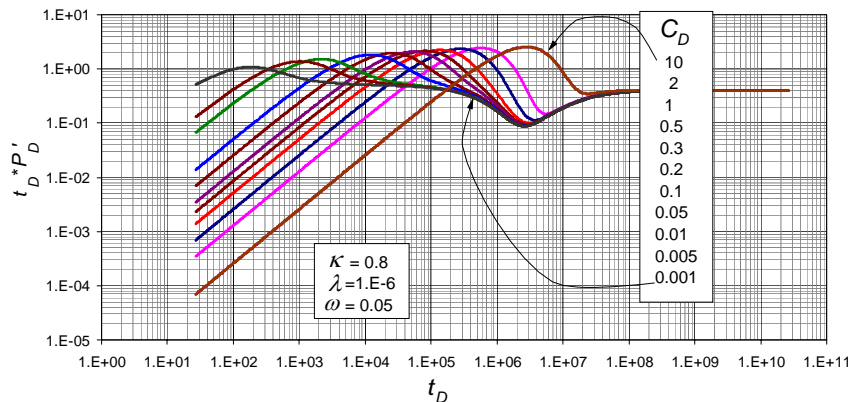


Figure-6. Effect of wellbore storage coefficient on the trough of the pressure derivative.



4. INFLUENCE OF WELLBORE STORAGE COEFFICIENT

As seen in Figure-6, the minimum value of the pressure derivative is affected by wellbore storage when $C_D \geq 0.2$ for $\kappa = 0.8$, $\lambda = 1 \times 10^{-6}$ and $\omega = 0.05$. This research also concludes that the minimum pressure derivative (trough) is not affected by wellbore storage effects for any value of ω only if the wellbore storage coefficient is not greater than the values provided in Table-3 for a given value of λ .

Table-3. Conditions for effects of wellbore storage on the minimum pressure derivative.

κ	C_D			
	$\lambda = 10^{-4}$	$\lambda = 10^{-5}$	$\lambda = 10^{-6}$	$\lambda = 10^{-7}$
0.1	3.89E+01	3.11E+02	1.94E+03	1.94E+04
0.2	3.89E+01	3.11E+02	1.94E+03	1.94E+04
0.3	3.89E+01	3.11E+02	3.11E+03	2.33E+04
0.4	7.77E+01	7.77E+01	7.77E+03	3.85E+04
0.5	7.77E+01	7.77E+01	7.77E+03	7.77E+04
0.6	7.77E+01	7.77E+01	7.77E+03	7.77E+04
0.7	7.77E+01	7.77E+01	7.77E+03	7.77E+04
0.8	7.77E+01	7.77E+01	7.77E+03	7.77E+04
0.9	1.55E+02	1.55E+03	7.77E+03	7.77E+04
0.99	1.55E+02	7.77E+02	7.77E+03	7.77E+04

Tiab, Igbokoyi and Restrepo (2007) presented Equations 16 to 19 to correct the minimum for the influence of wellbore storage effects.

$$(t^* \Delta P')_{min} = (t^* \Delta P')_{r2} + \frac{(t^* \Delta P')_{min,o} - (t^* \Delta P')_{r2} [1 + 2D_1 D_2]}{1 + D_2 \left[\ln \left(\frac{C}{(\phi c_i)^* h r_w^2} \right) + 2s - 0.8801 \right]} \quad (16)$$

where

$$C = \left(\frac{qB}{24} \right) \frac{t}{t^* \Delta P'} \quad (17)$$

$$D_1 = \left[\ln \left(\frac{qB t_{min,o}}{(t^* \Delta P')_{r2} (\phi c_i)^* h r_w^2} \right) + 2s - 4.17 \right] \quad (18)$$

$$D_2 = \frac{48.02C}{qB} \left(\frac{(t^* \Delta P')_{r2}}{t_{min,o}} \right) \quad (19)$$

Observe that Equation 18 considers the second radial flow regime which for that corresponds to the fracture net permeability. For the double-permeability case, this value is smaller since the matrix permeability forces the second radial flow to have a smaller pressure derivative value than the first radial flow pressure derivative.

5. SYNTHETIC EXAMPLES

5.1. Example-1

Figure-7 presents the pressure and pressure derivative data for a simulated test run with the information given in the third column of Table-1. It is requested to validate the equations for estimating the double-permeability reservoir parameters.

Solution

The following information was read from Figure-7:

$$(t^* \Delta P')_{min} = 12.3154121 \text{ psi } t_{min} = 7.048574 \text{ hr } (t^* \Delta P')_{r2} = 57.62287 \text{ psi}$$

Equations 13, 14 and 15 were used to estimate values of $\kappa = 0.7174$, $\omega = 0.4017$ and λ of 1.046×10^{-5} with relative deviation errors of 2.49, 0.4324 and 4.585 %, respectively. This demonstrates that the developed equations provide values within a reasonable range of error.

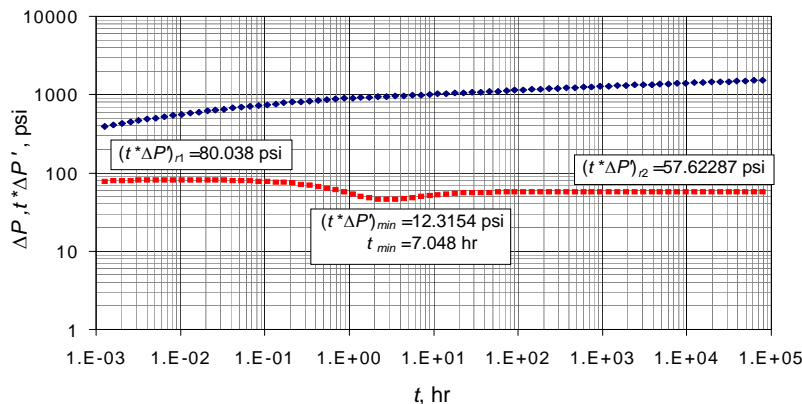


Figure-7. Pressure and pressure derivative log-log plot for example-1.

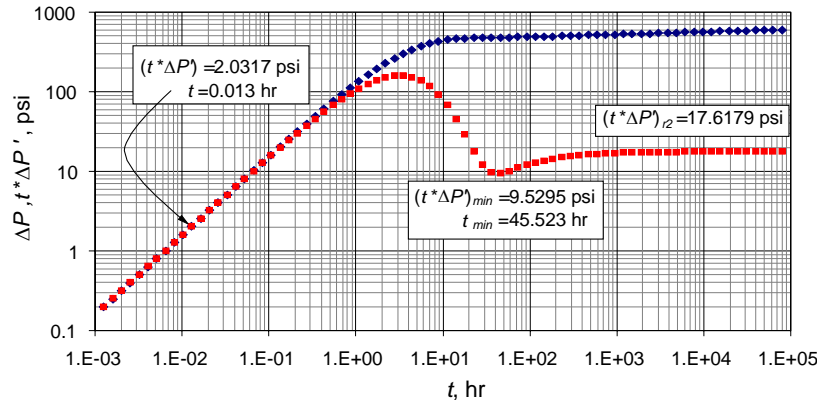


Figure-8. Pressure and pressure derivative log-log plot for example-2.

5.2. Example-2

Figure-8 also presents pressure and pressure derivative data generated with the information taken from the fourth column of Table-1. The purpose of this example is to validate Equations 16 to 19 to estimate the influence of the wellbore storage coefficient on the minimum value of the pressure derivative.

Solution

The following information was obtained from Figure-8.

$$(t^* \Delta P')_{min} = 9.5295 \text{ psi} \quad t_{min} = 45.523 \text{ hrs}$$

$$(t^* \Delta P')_{r2} = 17.6179 \text{ psi} \quad (t^* \Delta P')_{min} = 6.2176 \text{ psi (value without wellbore storage effects)}$$

Using Equation 16, Tiab *et al.* (2007), a value of 8.2417 psi is obtained for the corrected value of the minimum pressure derivative which represents a deviation error of 32.6% compared to the minimum when no wellbore storage was considered. However, if the first (masked) radial flow pressure derivative is estimated using the input fracture network permeability with Equation 2.7 from Tiab (1993) its value corresponds to 6.505 psi providing a deviation error of 4.62% which makes the solution more attractive.

6. ANALYSIS OF RESULTS

Only two examples are presented for space reasons. However, the obtained results provide low deviation values for the double-permeability parameters as compared to the input simulation values which confirm that the developed methodology works well. On the other side, using the correction of the minimum pressure derivative as proposed by Tiab *et al.* (2007) and error of 32.55% is obtained. However, that correction was given assuming that the value of the pressure derivative during the second radial flow regime is replaced by the first one which is masked but can be estimated from Equation 2.7 from Tiab (1993) using the input permeability. Under this situation the deviation error reduces to 4.62% which allows to recommend the above mentioned correction.

CONCLUSIONS

New expressions to estimate the interporosity flow parameter, λ , the dimensionless storage coefficient, ω , and the flow capacity ratio, κ , were developed and verified using characteristic points read from the pressure and pressure derivative plot for cases of no wellbore storage. The correction of the minimum pressure derivative provided by Tiab *et al.* (2007) may be used if the masked radial pressure derivative occurring before the transition period can be estimated from the network permeability.

ACKNOWLEDGMENTS

This work is dedicated to the second author James Vega (RIP) who passed away the day this work was completed.

REFERENCES

- Barenblatt G.I., Zheltov I. P. and Kochina I. N. 1960. PMM (Soviet Applied Mathematics and Mechanics). 24: 852.
- Bremer R.E., Winston H. and Vela S. 1985. Analytical Model for Vertical Interference Testing Across a Low-Permeability Zone. SPE Journal. pp. 407-418.
- Ehlig-Economides C. and Ayoub J.A. 1986. Vertical Interference Testing Across a Low-Permeability Zone. SPE Formation Evaluation. pp. 497-510.
- Hill A.C. and Thomas G.W. 1985. A New Approach for Simulating Complex Fractured Reservoirs. Paper SPE 13537 presented at the SPE 1985 Middle East Oil Technical Conference and Exhibition held in Bahrain. pp. 11-14.
- Engler T. and Tiab D. 1995. Analysis of pressure and pressure derivative without type curve matching, 4. Naturally fractured reservoirs. Journal of petroleum science and Engineering. 15 (1996) 127-138.



Tiab D., Igbokoyi A. and Restrepo D. 2007. Fracture Porosity from Pressure Transient Data. Presented at the International Petroleum Technology Conference held in Dubai, U.A.E. 4-6 December 2007. 8-9.

Wellbore Storage. Journal of Petroleum Science and Engineering. 12: 171-181. Also Paper SPE 25423, Production Operations Symposium held in Oklahoma City, OK. pp. 203-216.

Tiab D. 1993. Analysis of Pressure and Pressure Derivative without Type-Curve Matching: 1- Skin and

Warren J. and Root P. 1963. The Behavior of Naturally Fractured Reservoirs. SPE Journal, September.

NOMENCLATURE

B	Oil volume factor, rb/STB
c_t	System compressibility, 1/psi
C	Wellbore storage coefficient, bbl/psi
C_D	Dimensionless Wellbore storage coefficient referred to the layer production
C_{DV}	Dimensionless Wellbore storage coefficient referred to the total system
h	Formation thickness, ft
k	Permeability (horizontal), md
k_v	Vertical permeability, md
K_0, K_1	Bessel functions, second type
K_1^0	Bessel functions ratio
Kte	Constant the graphical λ determination
ℓ	Laplace transform variable
P	Pressure, psi
P_w	Well pressure, psi
P_D	Dimensionless pressure
q	Flow rate, BPD
r	Radius, ft
r_D	Dimensionless radius
r_e	External radius, ft
r_w	Wellbore radius, ft
s	Skin factor
t	Time, hr
t_D	Dimensionless time
t_{Dmin}	Dimensionless time at the minimum point
t_{min}	Time at the minimum point, hr
t_{DV}	Dimensionless time referred to the total system
$t_D^*P_D'$	Dimensionless pressure derivative
$t^*\Delta P'$	Pressure derivative, psi

Greek

ω	Dimensionless storage coefficient
ϕ	Porosity, fraction
λ	Interporosity flow parameter
κ	Capacity flow ratio
μ	Oil viscosity, cp

Suffices

1	Zone 1 properties (Fracture)
2	Zone 2 properties (Matrix)
D	Dimensionless
DV	Dimensionless vertical
DH	Dimensionless horizontal
i	Properties of zone i
min	Minimum
r	Radial
w	Well